RADIATION EFFECTS ON SILVER AND ZINC
BATTERY ELECTRODES. III.
Interim Report
October 1965 to January 1966
Prepared for
Jet Propulsion Laboratory
Under Contract No. 951109

N66-23762
(ACCESSION NUMBER)   (THRU)

39
(PAGES)

(CODE)

CR-74240
(NASA CR OR TMX OR AD NUMBER)

03
(CATEGORY)

ATOMICS INTERNATIONAL

A DIVISION OF NORTH AMERICAN AVIATION, INC.

RADIATION EFFECTS ON SILVER AND ZINC
BATTERY ELECTRODES. III.
Interim Report
October 1965 to January 1966
Prepared for
Jet Propulsion Laboratory
Under Contract No. 951109

By

M. M. NICHOLSON
H. L. RECHT
G. SCHLESINGER
W. A. McCOLLUM

ATOMICS INTERNATIONAL

A DIVISION OF NORTH AMERICAN AVIATION, INC.

MARCH 21, 1966

CONTENTS

TABLES

FIGURES

I. SUMMARY

The investigation of silver electrodes in experimental cells with cadmium counter electrodes was continued, with emphasis on the improvement of precision in the discharge capacity and gas evolution data. Steps have been taken for the closer standardization of discharge current density and depth of the conditioning cycle, for the reduction of ohmic drop effects in the recording and current control circuits, and for the establishment of a well-defined gas atmosphere before the irradiation step.

In closely matched cells at 90% state of charge, with capacity limited by the silver electrode, a capacity increase of 15% ($\pm$3%) was observed for the system receiving 7×10^7 rads (H_2O) of Co^{60} gamma radiation, while an increase of 12% ($\pm$2%) was observed for the control cell maintained at the same temperature. Further work will be required to ascertain the magnitude of radiation effects on the silver electrode capacity.

Hydrogen was again detected in irradiated cells, and it was shown that a minor quantity of this product originated from the polystyrene cell liner and/or the electrolyte solution in the absence of electrodes.

In future work, procedures will be developed for the study of secondary zinc electrodes. Major variables of interest for both electrodes are state of charge, total radiation dose, irradiation rate, and cycle depth.

II. INTRODUCTION

Batteries on space vehicles are exposed to various types of radiation from cosmic rays or the Van Allen belt. Nickel-cadmium and silver-zinc batteries received radiation doses of approximately 10^6 rads (H_2O) on the SNAP 10A mission. Damage from gamma rays is incipient at this level in the nickel-cadmium system.[1]

Recent work in this program on the silver-zinc system in 40% potassium hydroxide electrolyte has revealed two principal effects of gamma radiation: (a) loss of material from the silver electrode[2] and (b) evolution of hydrogen in cells containing silver test electrodes and cadmium counter electrodes. A change in coulombic capacity of the silver electrode during irradiation could not be excluded, but more precise capacity data were needed to refute or confirm that possibility.

III. EXPERIMENTAL

A. CELLS

Stainless steel cells with polystyrene liners, which have been described previously,[2] were used in this investigation. The steel cases were equipped with Swagelok Quick-Connect fittings to facilitate the removal of samples for gas analysis. The polystyrene liners were the three-compartment type, with fritted quartz separators.[2] The plastic partitions and bottoms for such cells were originally constructed by hand from polystyrene sheet; more recently these parts were machine fabricated for better uniformity and ease of assembly.

B. ELECTRODES

As in the preceding report period, the test electrodes were silver battery cathodes from Yardney Electric Company, cut to one-half their original size to provide the appropriate discharge capacity.[2] The counter electrodes were again of cadmium, removed from Union Carbide N75 sealed nickel-cadmium batteries and trimmed to fit the cell. Two cadmium electrodes, connected in parallel, were placed on opposite sides of the limiting silver electrode. The working electrodes were separated by quartz frits.

A new reference electrode designed for radiation work was constructed and evaluated for recording purposes during this quarter. The electrode was housed in a polystyrene container with a Nylon wick salt bridge, as shown in Fig. 1. The electrochemical system was $Hg/HgO/40\%$ KOH; the same

PLATINUM

POLYSTYRENE
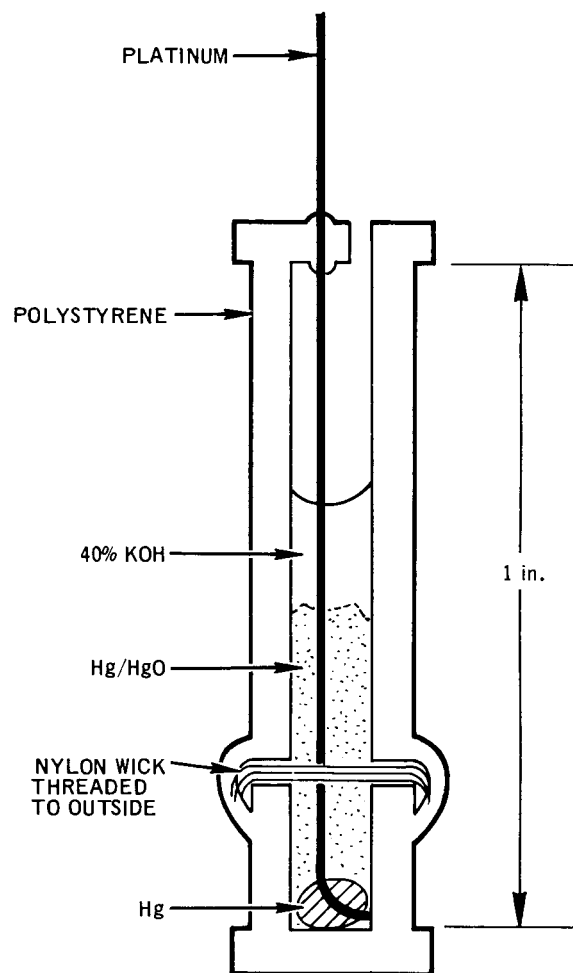
40% KOH

Hg/HgO

NYLON WICK
THREADED
TO OUTSIDE

Hg

1 in.

Figure 1. Reference Electrode

design would be applicable to other couples such as $Ag/Ag_2O/40\%$ KOH. The Nylon thread appeared to provide adequate chemical isolation, but it introduced a high impedance into the reference electrode circuit. For use with recording or control circuitry, this high impedance source of reference potential was converted to a low impedance source by the voltage follower scheme described in the next section.

C. ELECTRICAL CIRCUITS

1. Electrochemical Measurements

Brief descriptions of the automatic cycling and capacity measuring equipment were given in earlier reports.[2,3] Schematic diagrams of the two types of apparatus are shown in Figs. 2 and 3, respectively. The 15-minute clock provides a cycle of four phases, each of 15 minutes duration: open circuit - charge - open circuit - discharge. This shallow cycling process is applied in the preconditioning and irradiation steps. One cycling unit is used in conjunction with the radiation source; the other remains in the laboratory with the control cell.

The capacity measuring system operated by the 8-hour clock sends a constant discharging current through the cell as long as its total potential is above a preset lower limit. When this limit is reached, the cell is automatically held at essentially constant potential for the remainder of the 8-hour period by intermittent discharging as the cell tends to recover on open circuit. Analogous control at the upper voltage limit occurs in the charging mode. Thus, the capacity of two cells can be determined by the use of a common current source. Figure 4 shows a
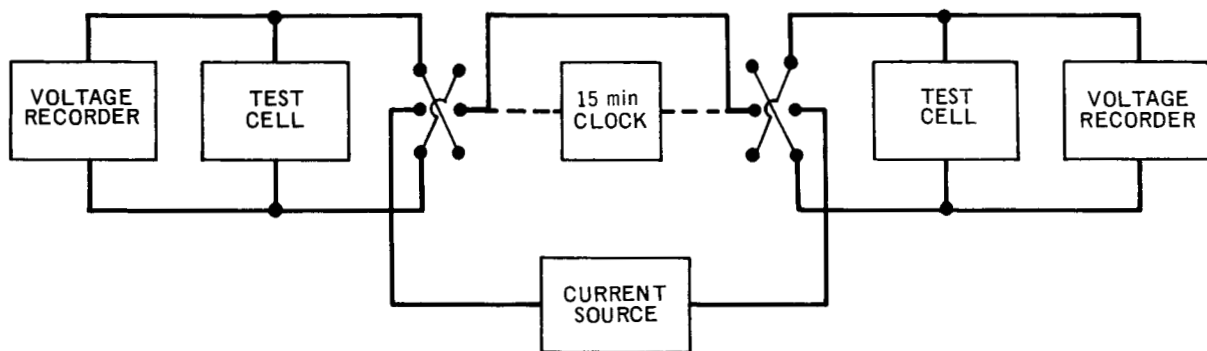
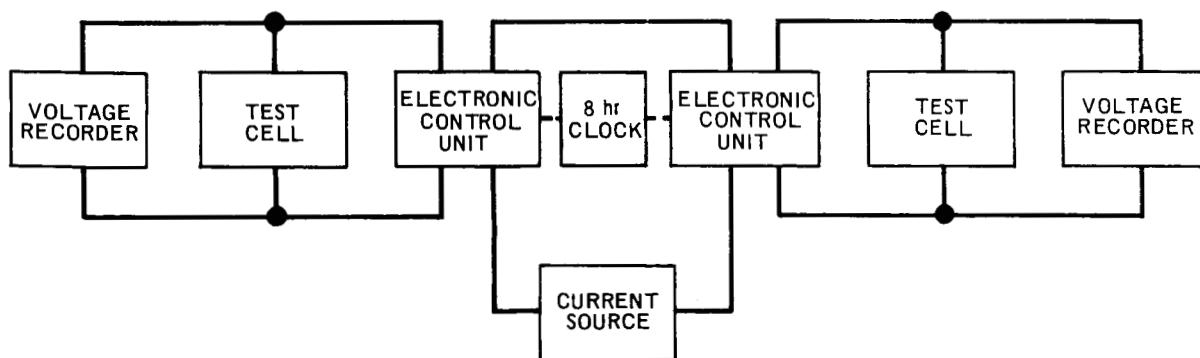Figure 2. Schematic Diagram of Cycling Circuit

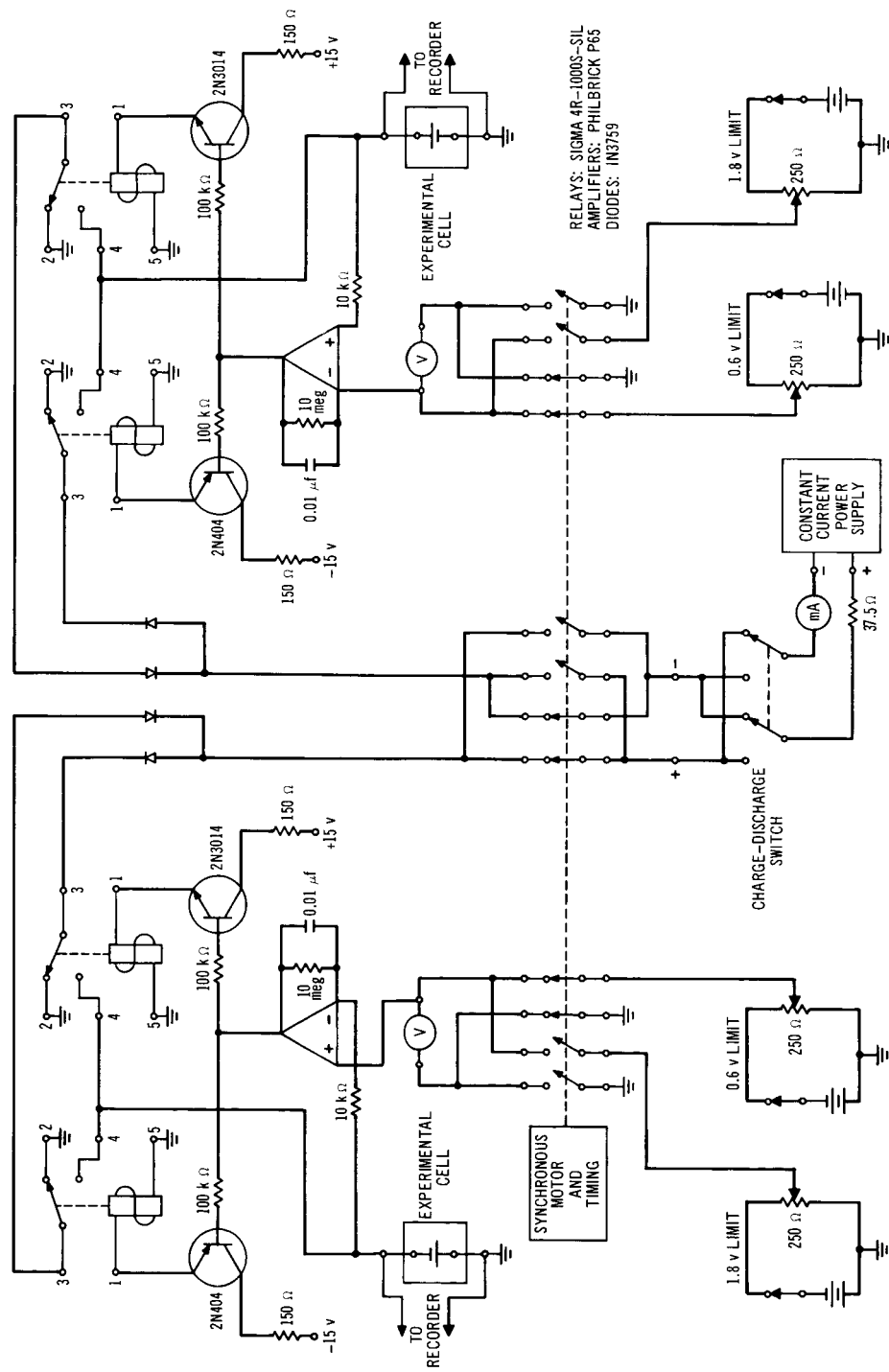Figure 3. Schematic Diagram of Capacity Measuring Circuit

Figure 4. Capacity Measuring Circuit

detailed circuit diagram of the present capacity measuring system for two test cells. The equipment represented in this figure is available in duplicate, each unit having a dual-pen recorder for the display of potential-time functions.

A control problem arises in this system when the total cell potential includes an appreciable ohmic component. On discharge, for example, the total potential rises immediately after cessation of the current by an amount equal to the IR drop. The relay then receives a signal to apply the discharge current, which reestablishes the ohmic drop. The system therefore oscillates with a rapid off-on response of the cell current. This produces an undesired treatment of the test electrode and appears to cause some instability in the current source.

A proposed solution to this problem is based on the use of a reference electrode in the control circuit. This electrode would be placed within the test electrode compartment, where the ohmic drop is negligible. The potential of the test electrode would also be recorded against the reference half-cell, rather than against the working counter electrode, to obtain more definitive electrochemical data. Construction of the reference electrode was described in the preceding section.

The voltage follower circuit for incorporating this electrode into the recording and control circuits is shown in Fig. 5. In this configuration, the operational amplifier serves to isolate the cell from the measuring and control systems by an effective impedance of the order of 10^8 ohms. The gain is unity, and the amplifier is non-inverting ($e_{out} = e_{in}$). The output

ANODE

EXPERIMENTAL
CELL

REF

CATHODE

COMMON

e_{in}

e_{out}

TO CURRENT
SOURCE

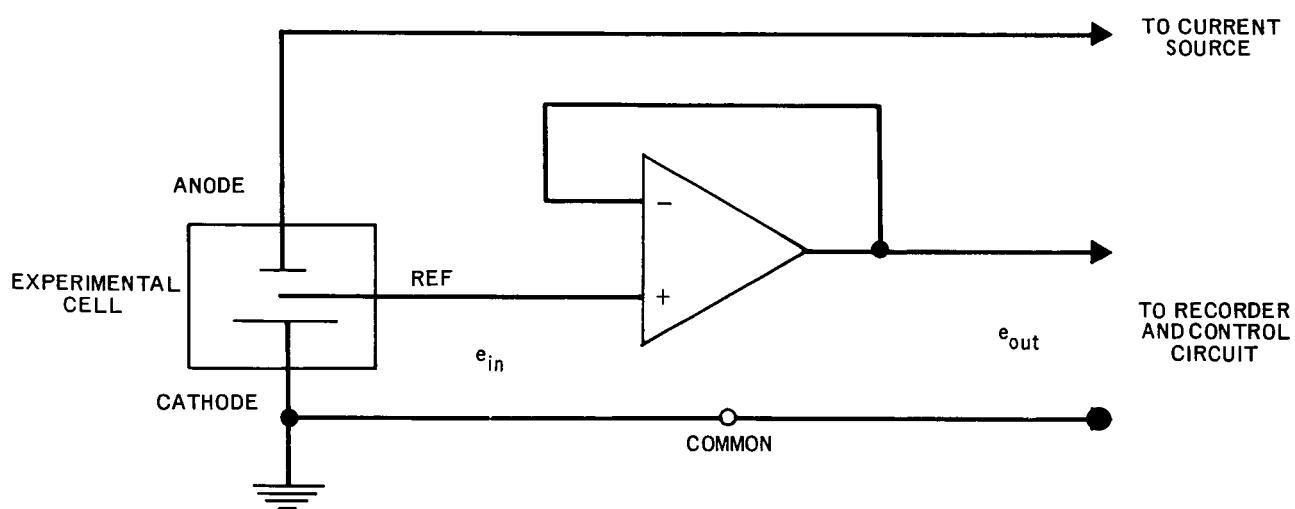TO RECORDER
AND CONTROL
CIRCUIT

Figure 5. Voltage Follower Circuit

of this amplifier should then be suitable for operating the existing detection system shown in Fig. 4, provided the grounding requirements are met. Experimental evaluation of this scheme is in progress, with a Philbrick P65AU amplifier as the voltage follower.

2. Pressure Measurements

A review of commercially available miniature pressure transducers was conducted prior to ordering replacements for the damaged units. Consolidated Electrodynamics Corporation Type 4-316-0001, with a range of ±25 psig still appears to be the most suitable for present requirements, although this model has shown some deterioration in previous work on this program. The sensor is a strain-gage which functions as a Wheatstone bridge. A circuit diagram for the pressure measuring system is given in Fig. 6.

D. GAMMA RADIATION SOURCES

The irradiations reported here were carried out in the Co^{60} gamma source that was used in previous work on this program.[2] The present rating of this source is 1.1×10^6 rads (H_2O) per hour. Installation of a more versatile Co^{60} source at Atomics International is scheduled for completion in February, 1966. The new source will provide a variable dose rate up to 2.5×10^6 rads (H_2O) per hour.

E. PROCEDURES

The electrochemical and irradiation procedures in the runs reported here were essentially those described in the preceding report.[2] The routine for a complete run is outlined in Fig. 7. The temperature of the control cell
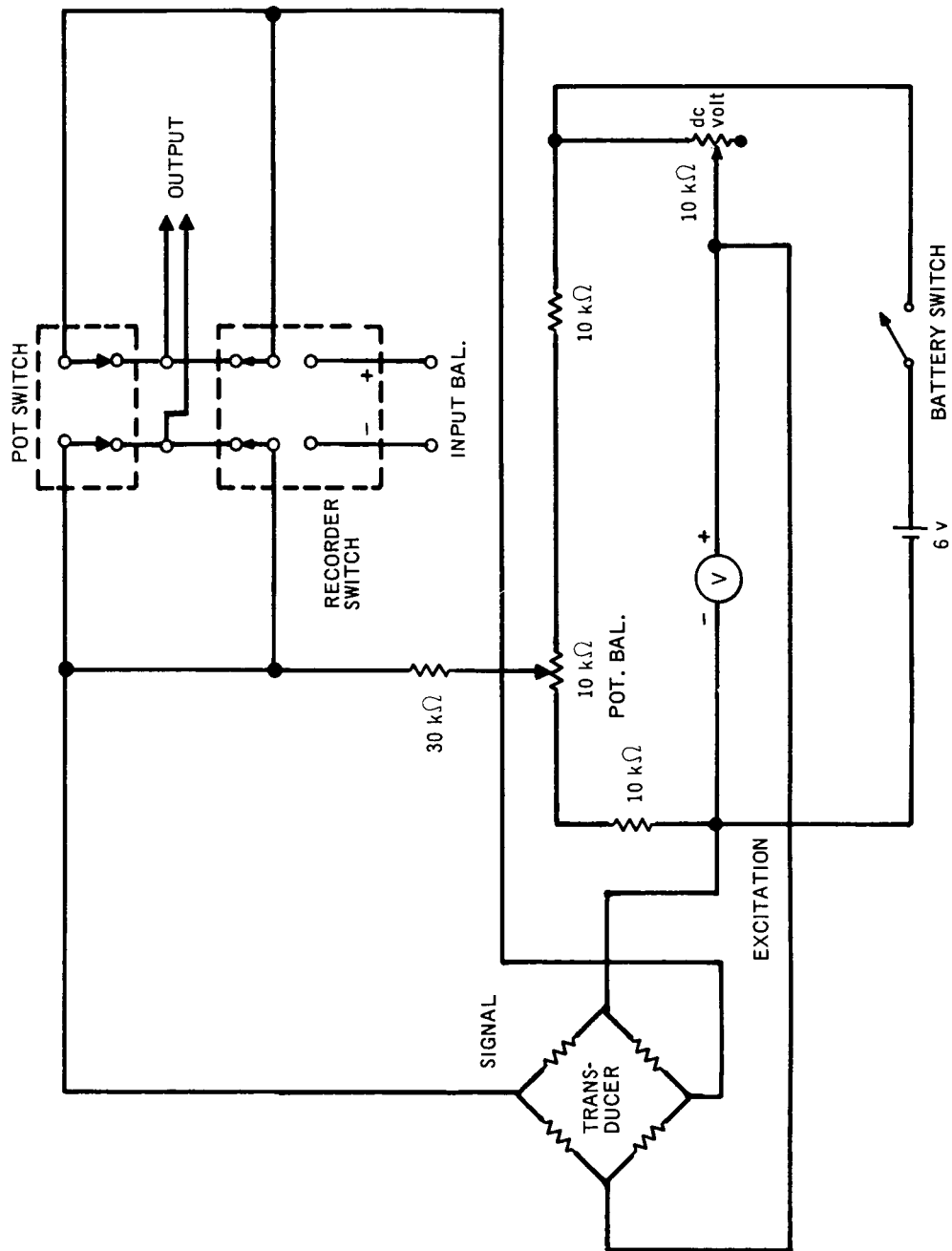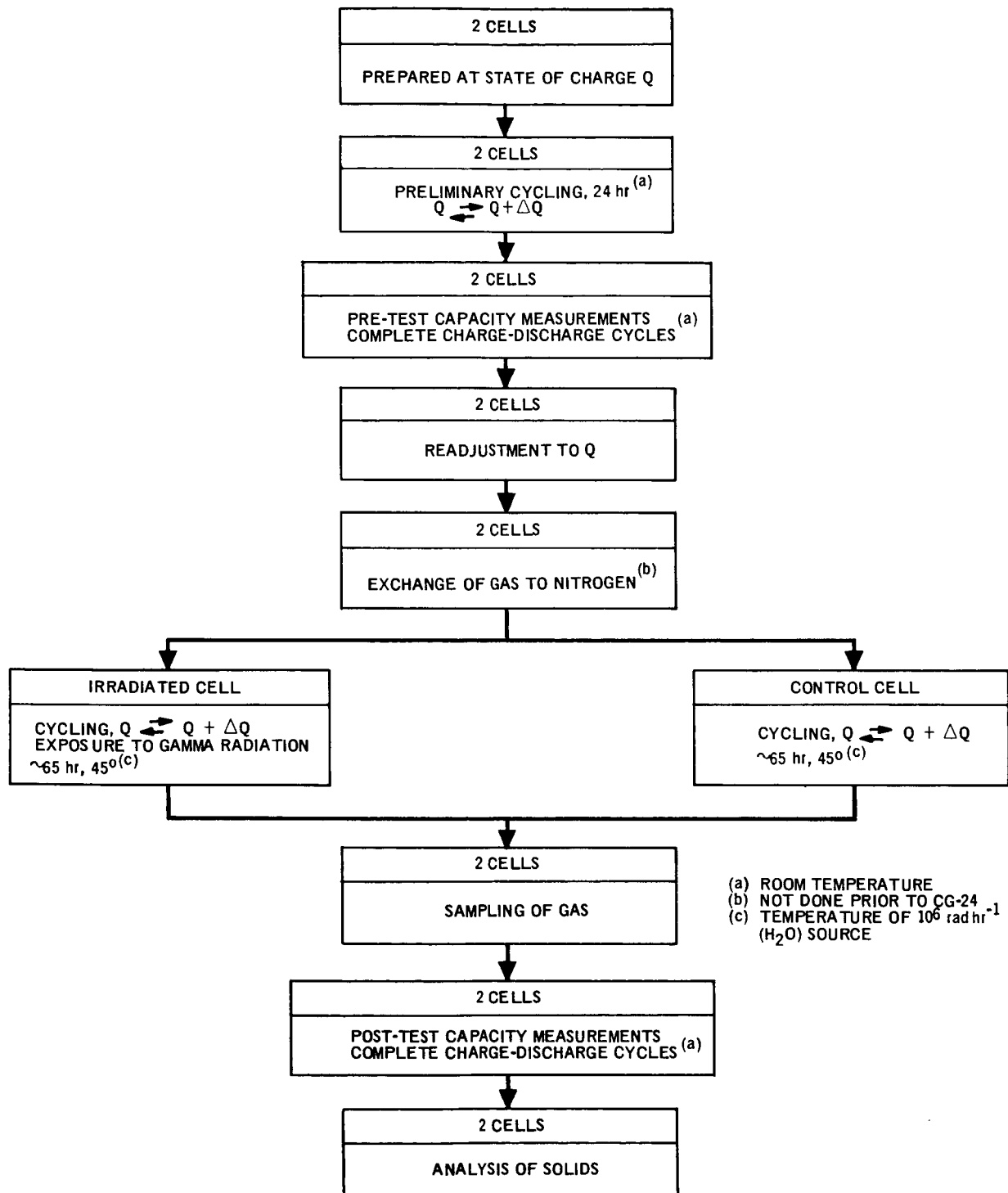
Figure 6. Pressure Measuring Circuit

Figure 7. Experimental Procedure for Silver Electrodes

was maintained at 45° to match that in the radiation source. Experimental changes incorporated since the previous report include:

(a) Machine fabrication of parts for the cell liners

(b) Use of an oil bath for more convenient temperature control of the nonirradiated cell

(c) Adjustment of the capacity measuring current* to 7.25 ma cm^{-2}

(d) Selection of the cycling current to yield a more precise 5% state of charge increment in 15 minutes

(e) Preliminary cycling from the same state of charge as that used in the irradiation stage.

Gas analyses were performed by mass spectrometry. The simple gas exchange manifold depicted in Fig. 8 has been constructed for the establishment of a well-defined pre-irradiation atmosphere and for use in leak testing of the steel cell. The exchange manifold and helium leak detector were not available at the time of the work reported here; however, their use is planned on all future runs.

The presence of ohmic drop in the quartz frit separators was demonstrated in the following manner. Two reference electrodes of the Hg/HgO type were inserted in a used cell containing silver and cadmium electrodes and the 40% potassium hydroxide electrolyte. The potential difference between the two reference electrodes in several configurations was measured potentio-metrically with and without the passage of cell current at 46 ma on one

_____

*Approximately 100 ma total current for a cut silver electrode.
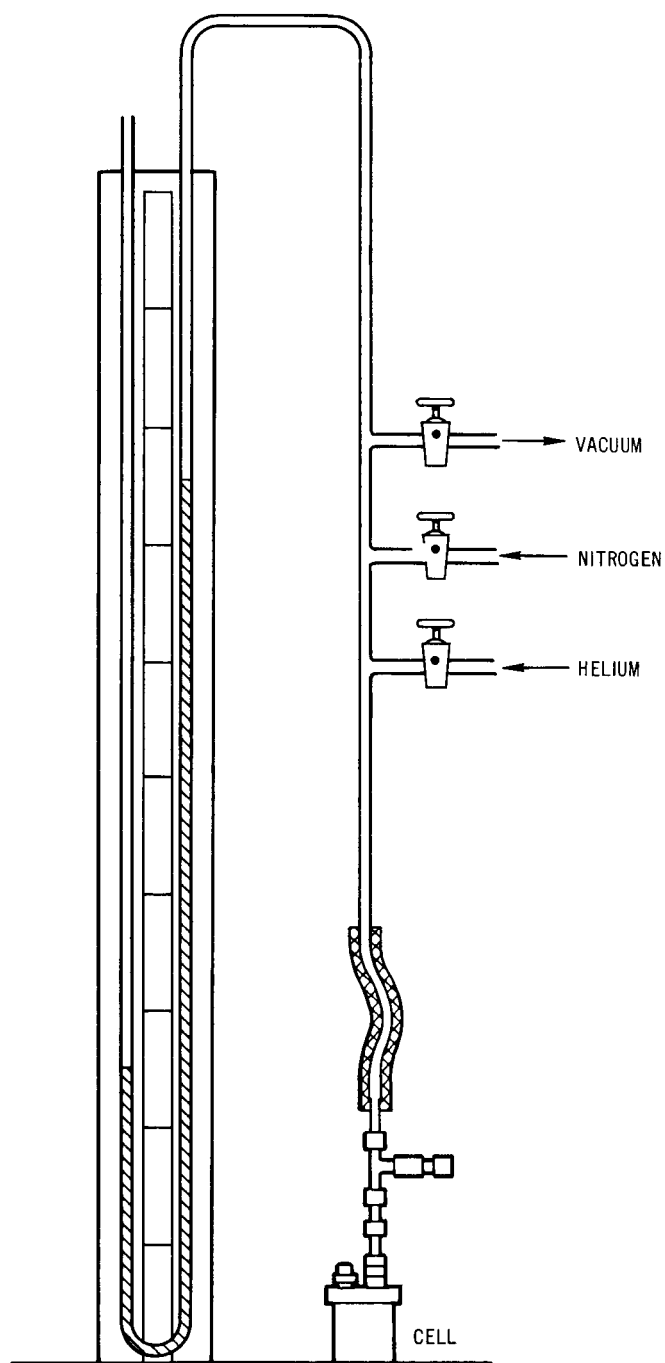
Figure 8. Gas Exchange System

face of the silver electrode. An ohmic drop of 150 mv was observed when the reference electrodes were separated by a frit. With both reference electrodes in the central compartment, their potential difference did not exceed 10 mv, even though they were placed in the current path. Thus, the resistance of the frit filled with electrolyte was approximately 3 ohms. This frit had been used in several irradiation runs and was subject to chemical attack by the alkaline solution. These measurements indicate that most of the ohmic drop in the experimental cells can be circumvented by means of a reference electrode.

IV. RESULTS

A. INSTRUMENTATION

The potential difference between the reference Hg/HgO and Ag/Ag_2O electrodes, recorded through the voltage follower, Fig. 5, was constant within 10 mv for 48 hours. The design in Fig. 1 should therefore be satisfactory for recording the potentials of test electrodes in this program.

The current output of the constant current power supply was monitored by recording across a series resistor during some of the capacity measurements. Variations over a 12-hour interval were typically of the order of 1% while both cells were within the cutoff limits. Variations of approximately 5% in the average output current were observed, however, when the cutoff system was in operation. The use of a reference electrode in the control circuit is expected to reduce this variation to essentially that inherent in the power supply design.

B. IRRADIATION RUNS

Conditions for the irradiation runs on silver electrodes are summarized in Table I. The irradiated and control cells were more closely matched and the current density and cycle depth more precisely controlled in Run CG-23 than in CG-22. Detailed capacity data are presented in Table II; analyses of gases and residual solids are given in Tables III and IV, respectively. Experimental difficulties prevented a silica analysis on the residue from Run CG-22. Table III also includes gas evolution data for a blank run on

a polystyrene cell liner containing 40% potassium hydroxide but no electrodes.

Characteristic shapes acquired by the potential-time curves during extended cycling at various charge levels have been mentioned previously.[2] Examples of these curves are shown in Figs. 9 and 10. The potentials were recorded between the silver and cadmium electrodes in each case; an ohmic component is included, therefore, in both the charge and discharge phases.
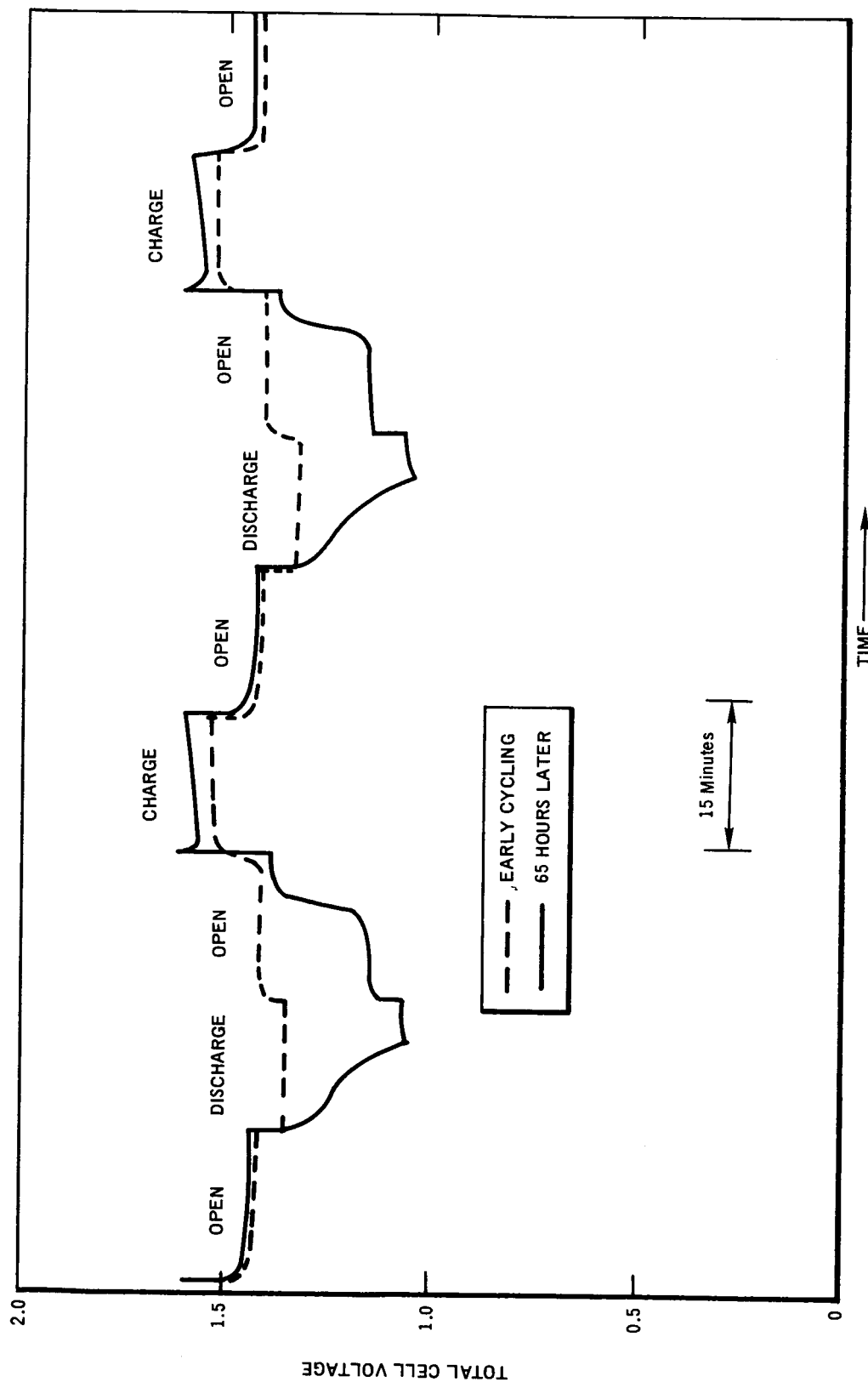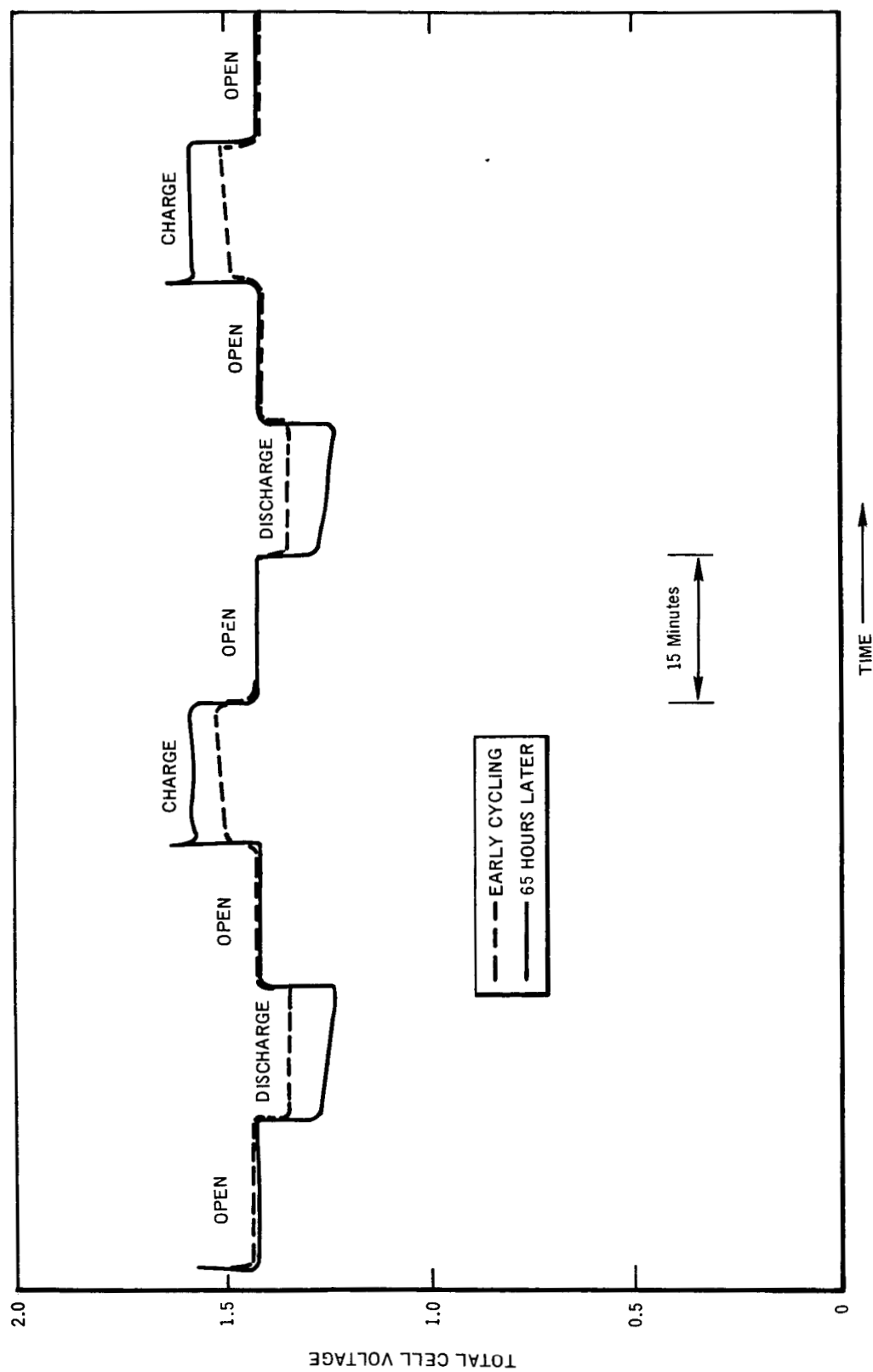
Figure 9. Cycling at 60-65 Percent Charge

Figure 10. Cycling at 90-95 Percent Charge

V. DISCUSSION

A. RECENT RESULTS

The improvement of precision in the capacity and gas evolution measurements were major objectives during this quarter. To that end, some modifications of design and procedures were developed, and damaged equipment was repaired or replaced. The principal changes introduced into practice are listed under Procedure; others intended for future work are described within the Experimental section.

The capacity measurements reported in Table II show acceptable precision ($\pm$1% to $\pm$3%) among consecutive discharge cycles. The first cycle was omitted in computing the average capacity, since this value is dependent on the termination point in the preconditioning (shallow cycling) stage and possibly on other factors. In Run CG-22, the irradiated cell showed a capacity increase of 11% ($\pm$1%). A water leak prevented the determination of post-test capacity in the control cell for this run. In run CG-23, the irradiated cell increased 15% ($\pm$3%) in capacity while the control cell increased 12% ($\pm$2%) during the same time. In previous runs at 90% state of charge and the same radiation dose, changes from -16% to +15% were observed in irradiated cells, and from -7% to +15%, in control cells. Additional data with more precise control of conditions are still required to resolve the capacity changes caused by radiation, if any, from those associated with temperature, cycling, and other variables.

The gas evolution data, Table III, must be considered semiquantitative

because of sealing problems that existed in the steel cells. These difficulties are now being corrected with the aid of a helium leak detector. As in earlier work, hydrogen was evolved during the irradiation step. More hydrogen was detected in a silver-cadmium test cell than in the blank containing only the polystyrene liner and the electrolyte. The blank cell did produce significant amounts of both hydrogen and methane upon irradiation, however, in processes distinct from those involving the electrodes.

The solid material recovered from the silver electrode compartment of the control cell was consistent in quantity and composition with that obtained in earlier runs at 90% charge. Such losses, exclusive of silica, have ranged from 4 to 15 mg,[2] while 7 mg was observed here.

The irradiated cell in Run CG-22 showed a typical solid loss, including silica, of the order of 50 mg. In Run CG-23, the corresponding loss, including silica, was only 27 mg; corrected for silica content, it was 26 mg. As in previous work, silver metal was the major constituent of the solids from the silver electrode compartments of both cells.

The potential-time curves for shallow cycling over an extended time are of interest in electrochemical characterization of the system. Such curves for control cells at the beginning and end of the 65 hour cycling stage are shown in Figs. 9 and 10 for 60 and 90% states of charge. At 90%, the open circuit potential was essentially constant at 1.42 v over the entire cycling time. The increased separation of charge and discharge potentials that developed in later cycling appears to be caused primarily by ohmic drop.

The development of a spike on the charge segment and a negative slope on the discharge segment suggests a trend toward more severe kinetic control as the system ages. In the 60% run, Fig. 9, this effect was more pronounced, and a slow recovery was observed on open circuit following discharge.

Increased kinetic control might occur if part of the active surface were lost during the cycling stage, with a resultant increase in current density referred to the true surface area. A loss in active area could result from (a) recrystallization of the electrode materials or (b) blocking by adsorption. In either case, the increased polarization seen in 15 minutes of current flow was not reflected in the capacity determined by complete discharge. This is not surprising for two reasons: (a) the two silver oxides form as distinct phases without the retention of crystal geometry during anodic oxidation[4] and (b) surface active materials may desorb as the solid is consumed in the electrode reaction or as the potential reaches highly positive or negative values. These interpretations are tentative; it must be recalled that the cycling curves are recorded at 45°, while the capacities are measured at room temperature.

B. PLANS FOR FUTURE WORK

Additional data will be obtained on silver electrodes at 90% state of charge to check the precision and consistency of results. The indicated precautions will be taken for standardization of currents and control of conditions in the gas phase. The use of cadmium counter electrodes will be continued, pending the further investigation of secondary zinc electrodes.

Testing procedures will be developed for the zinc electrodes, using retentive wrappings and any other modifications of techniques that may be required to obtain satisfactory capacity data.

Major variables to be studied for both electrodes are state of charge, radiation dose, irradiation rate, and cycle depth. Experiments will be designed to characterize the gas evolution processes more specifically with respect to reaction sites and synergism between the silver and zinc electrodes.

ACKNOWLEDGEMENT

Dr. G. R. Argue was a consultant on this program during the present report period.

REFERENCES

1. Argue, G. R., H. L. Recht, W. A. McCollum and D. E. McKenzie, "The Effects of Radiation on Nickel-Cadmium Battery Electrodes," AI-65-66, Final Report, Jet Propulsion Laboratory Contract 450514, June 1963 to June 1965, Atomics International, a Division of North American Aviation, Inc., Canoga Park, Calif.

2. Argue, G. R., H. L. Recht and W. A. McCollum, "Radiation Effects on Silver and Zinc Battery Electrodes. II," AI-65-264, Interim Report, Jet Propulsion Laboratory Contract 951109, July, 1965 to October, 1965, Atomics International, a Division of North American Aviation, Inc., Canoga Park, Calif.

3. Argue, G. R., H. L. Recht and W. A. McCollum, "Radiation Effects on Silver and Zinc Battery Electrodes. I," AI-65-158, Interim Report, Jet Propulsion Laboratory Contract 951109, April 1965 to July 1965, Atomics International, a Division of North American Aviation, Inc., Canoga Park, Calif.

4. Wales, C. P., and J. Burbank, J. Electrochem. Soc., 112, 13 (1965)

TABLE I.   CONDITIONS FOR SILVER ELECTRODE RUNS

Run[a]	Silver Electrode Wt[b] g	Area[c] cm²	Volume of Electrolyte ml	Capacity Measurements Total Current ma	Current Density ma cm⁻²	Cycling Total Current ma	Depth of Cycle[d] %
CG-22							
Irradiated Cell	1.56	14.5	60	100	7.1	100	5.5
Control Cell	1.62	15.0	65	100	7.3	100	5.4
CG-23							
Irradiated Cell	1.65	15.3	~50	111	7.2₅	91	5.0
Control Cell	1.65	15.3	~50	111	7.2₅	91	5.0

(a) Both runs were at 90% state of charge, 1.1×10^6 rads (H_2O) hr^{-1} dose rate, 7.3×10^7 rads (H_2O) total dose

(b) Corrected for weight of leads, but including embedded silver grid

(c) Total projected area, including both sides

(d) In irradiation stage, based on pre-test capacity

TABLE II. SILVER ELECTRODE CAPACITY

Run	Initial State of Charge % of Capacity	Cycle	Irradiated Cell				Control Cell			
			Pre-Test Capacity amp-hrs	Δᵇ	Post-Test Capacity amp-hrs	Δᵇ	Pre-Test Capacity amp-hrs	Δᵇ	Post-Test Capacity amp-hrs	Δᵇ
CG-22	90	1	~0.32ᵃ	---	0.529ᵃ	---	---	---	---	---
		2	0.450	-0.007	0.508	0.000	0.462	-0.005	---	---
		3	0.458	+0.001	0.510	+0.002	0.448	-0.019	---	---
		4	0.462	+0.005	0.506	-0.002	0.490	+0.023	---	---
		Average	0.457 ± 0.004		0.508 ± 0.001		0.467 ± 0.016		---	
			Change + 11% (±1%)				Change ------ᶜ			
CG-23	90	1	0.484ᵃ	---	0.532ᵃ	---	0.485ᵃ	---	0.518ᵃ	---
		2	0.474	+0.018	0.536	+0.013	0.461	+0.004	0.529	+0.016
		3	0.451	-0.005	0.533	+0.010	0.457	0.000	0.518	+0.005
		4	0.444	-0.012	0.501	-0.022	0.453	-0.004	0.501	-0.012
		5	---	---	0.522	-0.001	---	---	0.503	-0.010
		Average	0.456 ± 0.011		0.523 ± 0.012		0.457 ± 0.003		0.513 ± 0.011	
			Change +15% (±3%)				Change +12% (±2%)			

(a) Omitted from average

(b) Δ = deviation from average

(c) Water leak in control cell holder

TABLE III. ANALYSES OF GASES AFTER IRRADIATION STAGE

Run	Gas Volume ml	Total Pressure mm Hg	Volume Percent					
			O_2	N_2	Ar	CO_2	CH_4	H_2
CG-23[a]								
Irradiated Cell	55.0	688	17.5	77.5	0.90	0.30	---	3.8
Control Cell	52.8	700	16.0	83.0	0.91	0.02	---	---
Blank								
Irradiated Cell	76.4	726	18.2	78.2	0.90	---	0.72	1.35
Control Cell	---[b]	---[b]	21.8	76.5	0.91	---	---	---

(a) 90% state of charge; 1.1×10^6 rads (H_2O) hr^{-1} dose rate; 7.3×10^7 rads (H_2O) total dose

(b) Containing only polystyrene liner and 40% KOH

TABLE IV. ANALYSES OF SOLIDS RECOVERED FROM SILVER ELECTRODE COMPARTMENT

Run[a]	Total Wt mg	Wt % SiO_2	Net Wt mg	Identified[b]	Wt Cd/wt Ag[c]
CG-22					
Irradiated Cell	46.8	---[f]	---	---	---
Control Cell[d]	---	---	---	---	---
CG-23					
Irradiated Cell	26.9	3	26.1	Ag,Cd(OH)$_2$	0.06
Control Cell	7.4	~5[e]	7.0	Ag	~0.1

(a) 90% state of charge; 1.1×10^6 rads (H_2O) hr^{-1} dose rate; 7.3×10^7 rads (H_2O) total dose

(b) X-ray diffraction; major constituent first

(c) X-ray fluorescence

(d) Water leak in control cell holder

(e) Insufficient sample; estimate $3 < \% \, SiO_2 < 10$

(f) Experimental difficulties prevented analysis